THE ASTROPHYSICAL JOURNAL, 551:1107–1118, 2001 April 20

PLANETARY COMPANIONS TO HD 12661, HD 92788, AND HD 38529 AND VARIATIONS IN KEPLERIAN RESIDUALS OF EXTRASOLAR PLANETS[1]

DEBRA A. FISCHER,[2] GEOFFREY W. MARCY,[2] R. PAUL BUTLER,[3] STEVEN S. VOGT,[4] SABINE FRINK,[5] AND KEVIN APPS[6]

Received 2000 July 19; accepted 2000 December 15

ABSTRACT

Precision Doppler observations at the Lick and Keck observatories have revealed Keplerian velocity variations in the stars HD 12661, HD 92788, and HD 38529. HD 12661 (G6 V) has an orbital period of 252.7 ± 2.7 days, velocity semiamplitude $K = 88.4 \pm 2.0$ m s^{-1}, and orbital eccentricity $e = 0.23 \pm 0.024$. Adopting a stellar mass of 1.07 $M_\odot$, we infer a companion mass of $M \sin i = 2.79$ M_J and a semimajor axis of $a = 0.79$ AU. HD 92788 (G5 V) has an orbital period of 326.7 ± 3.2 days, velocity semiamplitude $K = 99.9 \pm 2.4$, and orbital eccentricity $e = 0.30 \pm 0.06$. The adopted stellar mass of 1.06 $M_\odot$ yields a companion mass of $M \sin i = 3.34$ M_J and a semimajor axis of $a = 0.95$ AU. HD 38529 (G4 IV) has an orbital period of 14.3 ± 0.8 days, velocity semiamplitude $K = 53.8 \pm 2.0$ m s^{-1}, and eccentricity $e = 0.27 \pm 0.03$. The stellar mass of 1.4 $M_\odot$ sets $M \sin i = 0.77$ M_J, with a semimajor axis of $a = 0.13$ AU for this companion. In addition to the 14.3 day periodicity, the velocity residuals for HD 38529 show curvature over the three years of observations. Based on a measurement of Ca II H and K emission, all three stars are chromospherically inactive. Based on both spectral synthesis modeling and narrowband photometry, HD 12661, HD 92788, and HD 38529 all appear to be metal-rich stars, reinforcing the correlation of high metallicity in the host stars of gas giant extrasolar planets. We examine the velocity residuals to the Keplerian fits for a subsample of 12 planet-bearing stars that have been observed longer than two years at the Lick Observatory. Five of the 12 (Ups Andromedae, τ Boo, 55 Cnc, HD 217107, and HD 38529) exhibit coherent variations in the residual velocities that are consistent with additional companions. Except for Upsilon Andromedae, the source of the velocity variation remains speculative pending completion of one full orbit. GJ 876 exhibits residual velocities with high rms scatter (24 m s^{-1}), lacking identifiable coherence. The residual velocities for six of the 12 stars (51 Peg, 70 Vir, 16 Cyg B, ρ CrB, 47 UMa, and HD 195019) exhibit rms velocity scatter of $\sim$7 m s^{-1}, consistent with errors. The residual velocity trends suggest that known planet-bearing stars appear to harbor a distant ($>$3 AU) detectable companion more often than other stars in our planet survey.

Subject headings: planetary systems — stars: general

1. INTRODUCTION

Since 1995, about 50 extrasolar planets have been discovered as companions to solar-type stars (Marcy, Cochran, & Mayor 2000). All of these planets were discovered in high-precision Doppler surveys. This technique is most sensitive to massive planets with short orbital periods. The extrasolar planets that have been discovered to date have ranges from $M \sin i = 0.15$ to about 10 M_J, with orbital periods ranging from 3 days to a few years. Despite the fact that massive planets are easier to detect, the distribution of detected planets is strongly peaked toward the lowest detectable masses. Thus, it appears that low-mass planets are predominant in nature and that planet formation in primordial disks may be truncated at masses greater than about 10 M_J. The observation of a planet transit around the star HD 209458 (Charbonneau et al. 2000; Henry et al. 2000) confirmed the low-density, gas giant nature of the Doppler-detected extrasolar planets.

The first system of planets was recently discovered orbiting the star Upsilon Andromedae (Butler et al. 1999). The shortest-period planet in this system was discovered first (Butler et al. 1997), and the Doppler analysis immediately showed a residual velocity trend. However, three more years of data were required to map out one full orbital period for the outermost planet in this system. Residual velocity trends have also been noted for the star 55 Cnc (Marcy & Butler 1998), HD 168443 (Marcy et al. 1999; Udry, Mayor, & Queloz 2001), HD 187123 (Butler et al. 1998), and HD 217107 (Vogt et al. 2000). Verification of the Keplerian nature of these trends and identification of the orbital parameters await phase closure of the longer-period trends.

2. OBSERVATIONS

The Lick Observatory has a 12 yr time baseline of precision Doppler measurements for about 100 stars using the Hamilton spectrograph (Vogt 1987). The velocities that predate 1995 have poorer precision (generally 10 m s^{-1}) and larger rms scatter; however, these data are still quite useful for identifying moderate-amplitude, long-period velocity variations. In 1994 November, the Hamilton optics were upgraded, and the velocity precision improved to 3–5 m s^{-1} for bright, chromospherically inactive stars. Our

[1] Based on observations obtained at the Lick Observatory, which is operated by the University of California, and on observations obtained at the W. M. Keck Observatory, which is operated jointly by the University of California and the California Institute of Technology.

[2] Department of Astronomy, University of California at Berkeley, 601 Campbell Hall 3411, Berkeley, CA 94720; and Department of Physics and Astronomy, San Francisco State University, San Francisco, CA 94132; fischer@serpens.berkeley.edu.

[3] Department of Terrestrial Magnetism, Carnegie Institution of Washington, 5241 Broad Branch Road NW, Washington, DC 20015-1305.

[4] UCO/Lick Observatory, University of California at Santa Cruz, Santa Cruz, CA 95064.

[5] Center for Astrophysics and Space Sciences, University of California, San Diego, 9500 Gillman Drive, Code 0424, La Jolla, CA 92093-0424.

[6] Astronomy Centre, Physics and Astronomy Subject Group, University of Sussex, Falmer, Brighton, BN1 9QJ, UK.

standard stars have velocities with slopes less than 1 m s^{-1} yr^{-1} and rms scatter of $\sim$6 m s^{-1}. In 1998, more than 200 new stars were added to the Lick survey (Fischer et al. 1999).

The precision Doppler program was extended to the Keck Observatory in 1996 (Vogt et al. 2000). Over 500 stars are now monitored at Keck with Doppler precision of 2–4 m s^{-1}. The planet search programs at Lick and Keck each have a unique set of target stars. However, when a planet candidate is detected by one program, we often follow up with observations at the other observatory to increase phase coverage of the orbit.

Our Doppler technique makes use of an iodine cell to impose a grid of sharp reference lines on the stellar spectrum. In the analysis, a high signal-to-noise ratio (S/N) template spectrum without iodine is combined with a Fourier transform spectrometer iodine observation to model program observations of the star with iodine (Butler et al. 1996).

2.1. *HD 12661*

HD 12661 (HIP 9683) was added to the Lick sample in 1998. When scatter in the velocities suggested the presence of a companion, this star was immediately added to the Keck program. A total of 23 velocity measurements were obtained with the Lick 3 m telescope. On three nights, two consecutive velocities were averaged to provide a single velocity measurement for the star. Consecutive observations are typically made at Lick for faint stars or when the seeing is poor. Fifteen velocity measurements were obtained with the Keck 10 m telescope. The Lick and Keck velocities each have independent, arbitrary velocity zero points. A velocity shift of 13 m s^{-1} was applied to all of the Keck velocities to bring the Lick and Keck zero points into agreement. This velocity shift was determined by first comparing Lick and Keck velocities obtained within 12 hr of one another and then by adjusting the shift slightly to minimize the rms of the orbital fit for the combined data set. Table 1 lists the Julian dates, velocities, uncertainties, and the observatory where the measurements were obtained. The uncertainties stem primarily from photon statistics. The Keck spectra for this star have typical S/Ns of 300 with velocity error bars of 2–3 m s^{-1}, while the Lick spectra generally have S/Ns of 100 and error bars of 7–8 m s^{-1}.

HD 12661 is classified in most references (e.g., Simbad, Hipparcos) as a K0 star; however, the color, $B-V = 0.71$, is more consistent with a spectral type G6 V star. The Hipparcos parallax yields a distance of 37.2 pc for this $V = 7.43$ star.

Prieto & Lambert (1999) use the Hipparcos distance with evolutionary tracks to derive log $g = 4.43$, $M_V = 4.58$ mag, $T_{\rm eff} = 5754$ K, and $R = 1.096\ R_\odot$ (all of these parameters are also consistent with a spectral type earlier than K0). From spectroscopic analysis, we derive [Fe/H] $=$ 0.29 ± 0.05. This compares well with our estimate from Strömgren narrowband photometry, which yields [Fe/H] $=$ 0.32 ± 0.07. We derive a stellar mass of 1.07 $M_\odot$, which includes the effect of high metallicity.

Strong chromospheric activity is correlated with magnetic activity and motions in the photosphere of the star, which can produce quasi-periodic radial velocity variations (Saar, Butler, & Marcy 1998; Marcy et al. 2000). Core emission in the Ca II H and K and Ca IRT lines are monitored at Keck and Lick, respectively, as an activity indicator in all program stars. Core emission in the Ca II H and K lines is characterized by a pseudo–equivalent width, or *S*-index, analogous to the Mount Wilson H-K project (Baliunas et al. 1998). The *S*-index is then transformed to log $R'_{\rm HK}$, a ratio of the H-K flux to the bolometric flux of the star. This index is a good indicator of the level of chromospheric activity and a good predictor of the rotational period (Noyes et al. 1984) and approximate age of F, G, and K main-sequence stars (Baliunas et al. 1995). Figure 1 shows a spectral window centered on the Ca II H line for HD 12661 (*dotted line*) with the National Solar Observatory (NSO) spectrum overplotted (*solid line*). There is no apparent core emission. The derived S value (0.14) implies a rotation period of 36 days and a chromospherically quiet log $R'_{\rm HK} =$ -5.12. Such stars are intrinsically stable to $\sim$3 m s^{-1} (Saar et al. 1998). Low chromospheric activity is also correlated with low chromospheric variability and photometric stability (Radick et al. 1998).

A Lomb-Scargle floating mean periodogram of the velocities reveals a broad, strong peak at 253 days for the combined Lick and Keck data set. The best-fit Keplerian for the combined data set, shown in Figures 2*a* and 2*b*, yields an orbital period of 252.7 ± 2.7 days, a semi-amplitude $K = 88.4 \pm 2.0$ m s^{-1}, and an eccentricity of 0.23 ± 0.024. Our assumed mass of 1.07 $M_\odot$ for HD 12661

TABLE 1

Radial Velocities for HD 12661

Julian Date (−2,450,000)	Radial Velocity (m s^{-1})	Uncertainties (m s^{-1})	Observatory
1027.00105......	80.13	10.08	Lick
1154.67286......	−31.19	8.57	Lick
1155.74646......	−59.90	8.91	Lick
1170.82822......	−54.49	3.40	Keck
1171.72771......	−55.69	2.96	Keck
1172.83133......	−55.85	3.31	Keck
1173.85688......	−58.14	3.52	Keck
1206.66613......	−87.58	8.98	Lick
1226.75095......	−61.84	2.41	Keck
1227.74485......	−59.66	2.45	Keck
1228.72258......	−59.35	2.48	Keck
1445.01668......	−48.34	6.93	Lick
1445.99608......	−54.59	7.17	Lick
1446.99794......	−59.27	7.76	Lick
1498.79127......	−16.18	8.43	Lick
1501.74361......	−27.27	9.96	Lick
1533.77236......	77.04	6.74	Lick
1534.75244......	80.88	8.49	Lick
1535.71377......	82.67	6.06	Lick
1536.69256......	74.30	7.12	Lick
1539.73340......	76.06	6.72	Lick
1540.69929......	87.69	6.51	Lick
1550.75749......	106.54	2.53	Keck
1551.78363......	106.85	2.55	Keck
1552.78690......	107.69	3.45	Keck
1580.73242......	85.13	2.82	Keck
1581.79127......	83.27	2.85	Lick
1582.70565......	78.89	2.59	Keck
1583.71929......	82.24	2.31	Keck
1585.71510......	74.72	2.76	Keck
1750.97925......	−28.92	5.56	Lick
1752.98245......	−22.42	4.58	Keck
1757.05281......	−3.49	3.17	Lick
1774.97266......	22.38	4.19	Lick
1776.00116......	14.15	4.38	Lick

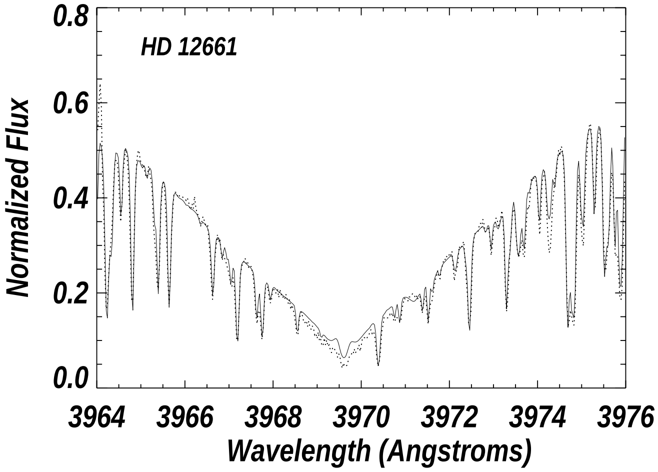

FIG. 1.—Spectrum of HD 12661 near the Ca II H line (*dotted line*) with the solar NSO spectrum overplotted (*solid line*). The lack of core emission indicates that HD 12661 is chromospherically inactive.

then implies a companion mass $M \sin i = 2.79$ M_J. The orbital elements for HD 12661 are summarized in Table 2. The rms to the fit of the Keplerian curve is 9.27 m s^{-1}, with a reduced χ^2 of 1.81. The residuals to the orbital fit show a linear trend, suggesting the presence of an additional companion.

2.2. *HD 92788*

HD 92788 was also added to the Lick sample in 1998. Twenty observations were obtained at Lick. On five occasions, consecutive velocities were averaged to yield a single velocity. Twelve observations of HD 92788 were obtained at Keck, and an offset of 6 m s^{-1} was applied to the Keck velocities in order to bring the Keck and Lick zero points into agreement. This offset was determined by comparing Lick and Keck velocities obtained within a few hours of each other and then adjusting the shift to minimize the rms scatter in the orbital fit. Table 3 lists the Julian dates, velocities, uncertainties, and the observatory where the measurements were obtained.

HD 92788 (HIP 52409) is classified as a G5 V star with a Hipparcos distance of 32.3 pc, $V = 7.31$, and $B-V = 0.694$. Using Hipparcos data (Perryman 1997) and stellar evolution models, Prieto & Lambert (1999) derive a mass of 0.97 $M_\odot$, $T_{\rm eff} = 5754$ K, $R = 1.05$ $R_\odot$, and $\log g = 4.41$ for this star. We measure a spectroscopic metallicity of [Fe/H] $= 0.22 \pm 0.05$, matching our estimate of [Fe/H] $= 0.24$ from Strömgren photometry. Accounting for metallicity, we estimate the stellar mass to be 1.06 $M_\odot$. The Ca H line (Fig.

TABLE 2

ORBITAL PARAMETERS

Parameter	HD 12661	HD 92788	HD 38529
P (days)	252.7 (2.7)	326.7 (3.2)	14.32 (0.8)
T_p (JD).............	2,451,542.5 (4.3)	2,451,734.5 (8.0)	2,451,565.7 (2.0)
e.....................	0.23 (0.024)	0.30 (0.06)	0.27 (0.03)
ω (deg)	323.1 (8.5)	272.0 (16)	90.9 (6.0)
K_1 (m s^{-1}).........	88.4 (2.0)	99.9 (2.4)	53.8 (2.0)
a (AU).............	0.79	0.95	0.13
$a_1 \sin i$ (AU).......	2.00×10^{-3}	2.85×10^{-3}	6.81×10^{-5}
$f_1(m)$ ($M_\odot$)..........	1.66×10^{-8}	2.91×10^{-8}	2.059×10^{-10}
$M_2 \sin i$ (M_J)	2.79	3.34	0.77
Observations[a]......	35	27	75
rms (m s^{-1})........	9.27	6.4	6.08
χ^2	1.81	0.97	1.3

NOTE.—Velocities obtained within a 2 hr period at Lick are averaged values, counted as a single observation.

[a] Number of observations from both Lick and Keck.

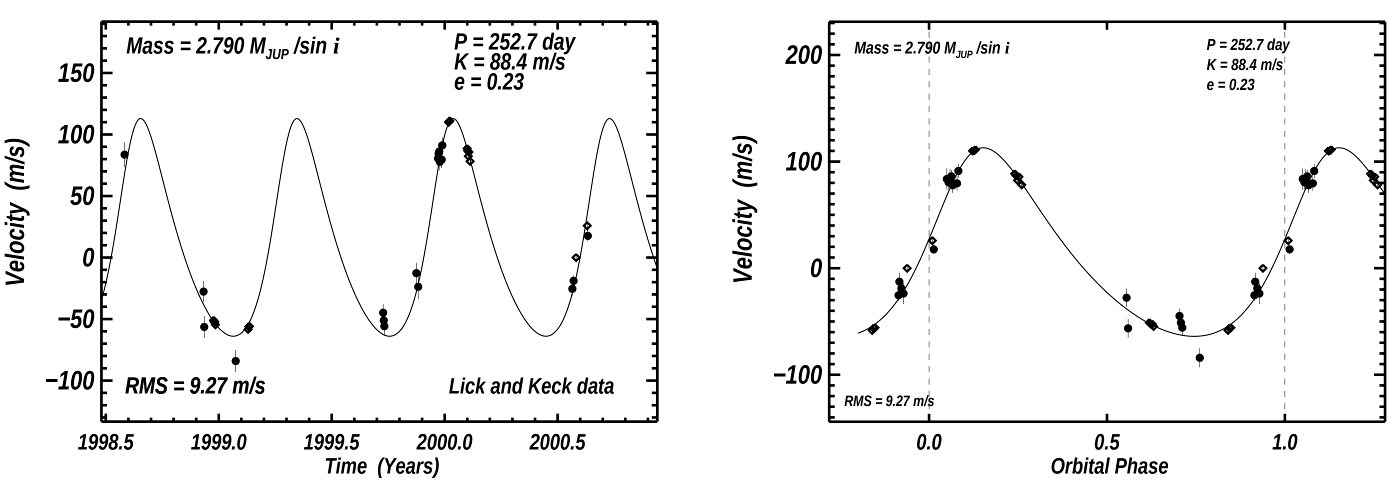

FIG. 2.—Combined Lick and Keck radial velocities as a function of (*left*) time and (*right*) phase for HD 12661. Lick observations are shown as circles, and the Keck data are plotted as diamonds. The solid line is the radial velocity curve from the best-fit orbital solution.

TABLE 3

RADIAL VELOCITIES FOR HD 92788

Julian Date (−24,50,000)	Radial Velocity (m s^{-1})	Uncertainty (m s^{-1})	Observatory
831.908	105.76	10.96	Lick
1242.887......	14.15	8.80	Lick
1298.758......	−64.34	9.03	Lick
1299.704......	−39.89	8.40	Lick
1300.717......	−36.10	9.82	Lick
1303.704......	−50.40	7.40	Lick
1534.077......	56.29	8.04	Lick
1535.090......	39.88	9.27	Lick
1536.054......	45.72	6.92	Lick
1536.965......	41.62	6.65	Lick
1540.086......	38.75	8.78	Lick
1541.005......	39.43	8.73	Lick
1552.106......	34.62	4.03	Keck
1553.034......	34.56	3.86	Keck
1581.979......	−4.51	3.55	Keck
1582.969......	0.00	3.32	Keck
1583.942......	2.88	3.23	Keck
1584.991......	−1.95	2.55	Keck
1585.962......	−1.89	3.50	Keck
1627.772......	−53.83	9.30	Lick
1628.738......	−49.67	7.26	Lick
1629.855......	−61.57	7.41	Lick
1678.910......	−79.45	5.17	Keck
1703.796......	−70.21	4.92	Keck
1705.795......	−66.89	4.94	Keck
1706.792......	−66.76	4.92	Keck
1755.737......	88.15	6.88	Keck

3) shows that this is a chromospherically quiet star. The activity-based rotation period is $P_{\rm rot} = 31.7$ days, and $\log R'_{\rm HK} = -5.04$.

A Lomb-Scargle floating mean periodogram of the radial velocities shows a strong peak at 327 days. A best-fit Keplerian to the combined Lick and Keck data (Figs. 4*a* and 4*b*) yields an orbital period of 326.7 ± 3.2 days, a semimajor amplitude of $K = 99.9 \pm 2.4$ m s^{-1}, and eccentricity $e = 0.30 \pm 0.06$, with an rms of 6.4 m s^{-1} and $\chi^2 = 0.97$. Adopting a stellar mass of 1.06 $M_\odot$, we derive a companion mass $M \sin i = 3.34\ M_{\rm J}$ and a semimajor axis $a = 0.95$ AU. The orbital parameters are summarized in Table 2. Queloz et al. (2001) have announced an independent detection of this system.

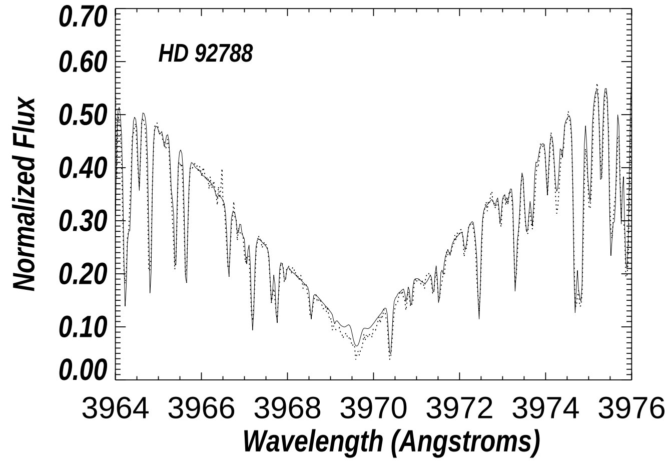

FIG. 3.—Ca II H line for HD 92788 (*dotted line*) with the solar NSO spectrum overplotted (*solid line*). The lack of emission indicates that this star is chromospherically quiet.

2.3. *HD 38529*

Observations of HD 38529 began in 1997 at Keck. When velocity variations were observed at Keck, this bright $V = 5.95$ star was added to the Lick sample in 1998 to increase phase coverage. A total of 25 observations were obtained at Keck, and 50 observations have been made at Lick. A velocity offset of −12 m s^{-1} was determined in the same manner described for HD 12661 and HD 92788 and applied to the Keck velocities to bring the Keck and Lick zero points into agreement. Table 4 lists the Julian dates, velocities, uncertainties, and the observatory where the data were obtained.

HD 38529 (HIP 27253) is classified as a G4 IV star, with $B-V = 0.773$. The Hipparcos distance of 42.4 pc sets $M_V = 2.81$ mag. Prieto & Lambert (1999) derive a mass of 1.39 $M_\odot$, $\log g = 4.13$, $T_{\rm eff} = 5370$ K, and radius $R = 2.82$ $R_\odot$. The Ca H and K lines provide evidence that this star is chromospherically quiet (Fig. 5). The measured S value suggests $P_{\rm rot} = 34.5$ days and $\log R'_{\rm HK} = -4.89$. However, these values are uncertain because the relation between $P_{\rm rot}$

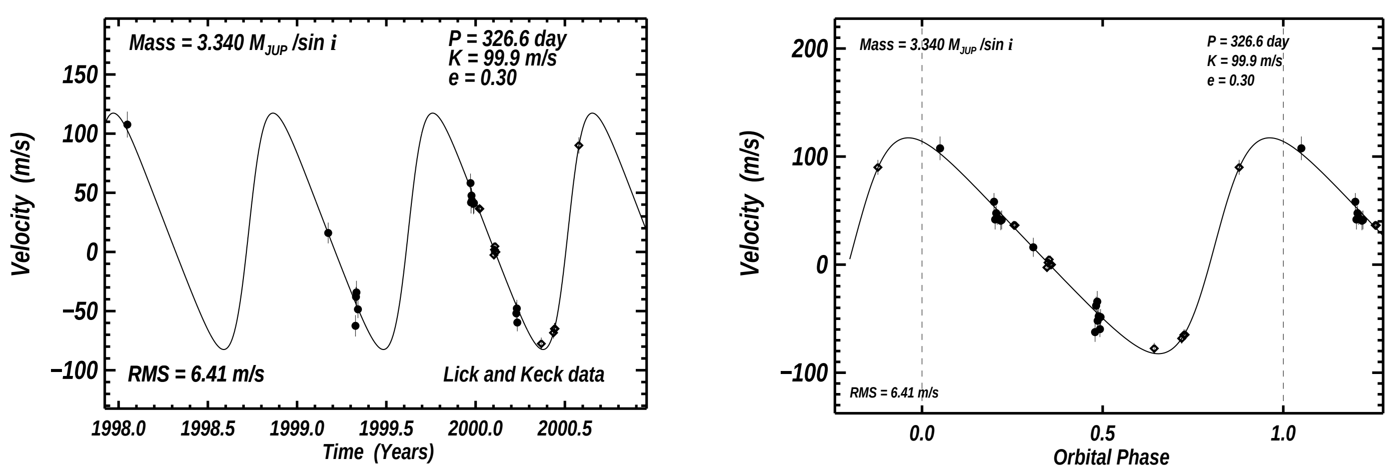

FIG. 4.—Combined Lick and Keck radial velocities as a function of (*left*) time and (*right*) phase for HD 92788. Lick observations are shown as circles, and the Keck data are plotted as diamonds. The solid line shows the theoretical Keplerian curve for the best-fit orbital solution.

TABLE 4

Radial Velocities for HD 38529

Julian Date (−2,450,000)	Radial Velocity (m s^{-1})	Uncertainty (m s^{-1})	Observatory
418.959	133.27	2.91	Keck
545.771	70.40	2.80	Keck
787.014	−15.36	2.99	Keck
807.062	−9.75	3.06	Keck
837.758	−74.15	2.82	Keck
838.784	−57.06	3.01	Keck
861.730	26.01	2.63	Keck
862.725	14.72	2.72	Keck
1073.059......	0.00	3.02	Keck
1101.015......	−5.88	7.08	Lick
1101.035......	−10.76	6.80	Lick
1102.015......	13.92	7.46	Lick
1102.032......	−1.32	7.74	Lick
1131.912......	22.69	7.20	Lick
1131.931......	16.69	7.42	Lick
1132.929......	36.21	6.61	Lick
1154.808......	−53.99	8.34	Lick
1170.895......	−25.43	3.06	Keck
1173.906......	−11.03	12.24	Lick
1173.928......	−9.22	16.04	Lick
1174.861......	36.91	9.73	Lick
1174.878......	11.83	11.16	Lick
1175.913......	10.87	8.05	Lick
1175.932......	31.50	8.19	Lick
1206.805......	7.41	8.01	Lick
1212.786......	−68.69	7.53	Lick
1213.786......	−56.29	9.12	Lick
1226.830......	−53.71	3.09	Keck
1227.758......	−45.31	2.96	Keck
1228.852......	−32.41	2.57	Keck
1229.774......	−25.86	2.98	Keck
1454.010......	−51.96	7.21	Lick
1454.031......	−48.62	6.62	Lick
1455.020......	−29.93	10.99	Lick
1455.040......	−19.78	10.77	Lick
1468.050......	−47.58	8.21	Lick
1468.963......	−38.93	6.51	Lick
1482.972......	−35.78	8.10	Lick
1482.994......	−20.00	9.25	Lick
1496.923......	−35.67	9.13	Lick
1496.942......	−43.08	13.03	Lick
1532.845......	59.82	6.19	Lick
1532.857......	64.22	6.42	Lick
1533.859......	80.49	5.17	Lick
1533.864......	82.53	4.81	Lick
1534.896......	84.76	6.93	Lick
1534.904......	77.05	8.11	Lick
1535.881......	58.67	4.77	Lick
1536.829......	27.50	5.62	Lick
1539.931......	−32.66	5.79	Lick
1540.867......	−14.33	6.03	Lick
1540.872......	−14.43	5.82	Lick
1543.791......	29.90	7.58	Lick
1546.832......	65.60	7.93	Lick
1550.879......	55.06	3.12	Keck
1551.909......	10.99	2.87	Keck
1552.857......	−14.13	2.64	Keck
1571.753......	5.86	7.02	Lick
1572.654......	24.51	6.67	Lick
1573.706......	34.03	13.29	Lick
1573.729......	41.61	18.75	Lick
1580.847......	1.95	2.71	Keck
1581.663......	−23.78	8.21	Lick
1581.713......	−12.01	6.89	Lick

TABLE 4—*Continued*

Julian Date (−2,450,000)	Radial Velocity (m s^{-1})	Uncertainty (m s^{-1})	Observatory
1581.757......	−11.82	3.03	Keck
1582.792......	−11.25	3.00	Keck
1583.913......	−1.53	3.24	Keck
1584.709......	−3.12	5.17	Lick
1584.712......	4.63	4.39	Lick
1584.784......	9.04	3.01	Keck
1585.909......	28.65	2.92	Keck
1593.798......	66.21	6.04	Lick
1607.720......	67.35	8.50	Lick
1607.742......	84.16	7.52	Lick
1629.655......	48.41	5.11	Lick

and log $R'_{\rm HK}$ to the *S*-index (Noyes et al. 1984) was calibrated with main-sequence stars. We have measured a spectroscopic metallicity of [Fe/H] $= 0.29 \pm 0.05$, which agrees with the narrowband photometric metallicity, [Fe/H] $= 0.23$ of G. Laughlin (2000, private communication).

A Lomb-Scargle periodogram of the velocities (Fig. 6) reveals a 14.3 day periodicity. However, there are nonlinear residual velocities to a 14.3 day Keplerian fit that suggest the presence of an additional companion with an orbital period of several years. To reduce confusion from this nonlinear residual trend, we modeled the 14.3 day Keplerian in a 5 month interval of data, sampled with high cadence. Even in this relatively short interval, there is an obvious linear trend. Allowing a linear trend of 100 m s^{-1} yr^{-1}, we model a short-period Keplerian velocity variation with an rms fit of 6.12 m s^{-1}, consistent with the typical velocity precision obtained at Lick for this star. This Keplerian, shown in Figure 7, yields a velocity amplitude of 53.8 m s^{-1}, an eccentricity of 0.27 ± 0.03, and $M \sin i = 0.77\ M_{\rm J}$. This orbital solution was then verified iteratively for the entire data set in the following way: We subtracted the 14.3 day Keplerian and modeled the residual velocity with a minimum-amplitude, 1500 day Keplerian. The longer-period theoretical Keplerian velocities were then subtracted from the data set, and the 14.3 day Keplerian was refitted using the entire 3 yr data set. The rms fit of the short-period companion increased to 12.7 m s^{-1} yr^{-1} when the entire 3

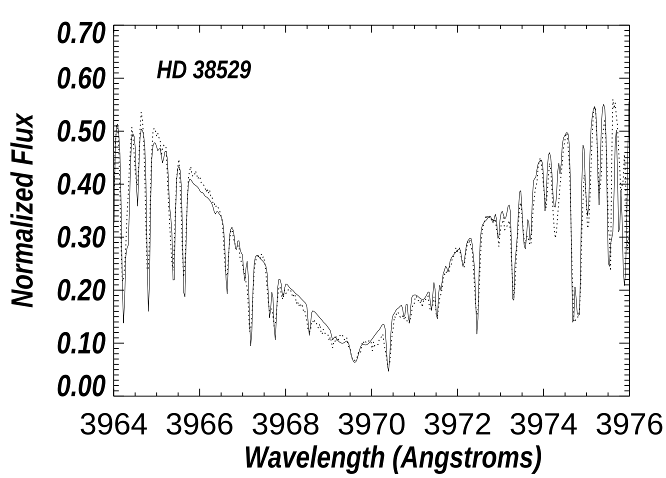

Fig. 5.—Ca II H line for HD 38529 (*dashed line*) with the solar NSO spectrum overplotted (*solid line*). This star is slightly evolved and appears to be chromospherically quiet.

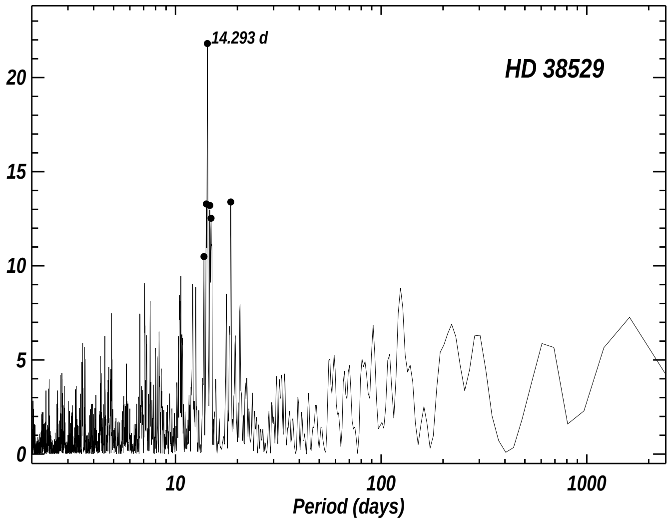

FIG. 6.—Periodogram of the combined set of Keck and Lick radial velocities for HD 38529, with a tall peak at 14.3 days.

yr data set was used. The reason for the poorer fit in the entire data set may originate from astrophysical sources, or it may signal an inadequate fit from our two assumed Keplerian solutions. Improvement in modeling awaits phase closure of the putative second Keplerian orbit. At this time, we adopt the orbital parameters found in the more robustly modeled 5 month interval.

We emphasize that the Keplerian nature of the long-period modulation (suggested by the fit in Fig. 8) cannot be established until at least one full orbital period is completed. If real, the true orbital period may be much longer than the suggested 6 yr period, and the mass of the putative second planet may substantially exceed the $M \sin i$ of 4 M_J estimated from this early fit. Indeed, HD 38519 has an acceleration solution in Hipparcos that is indicative of a companion with a period of the order of roughly 10 yr. In the Double and Multiple Systems Annex it is listed with accelerations in proper motions in right ascension and

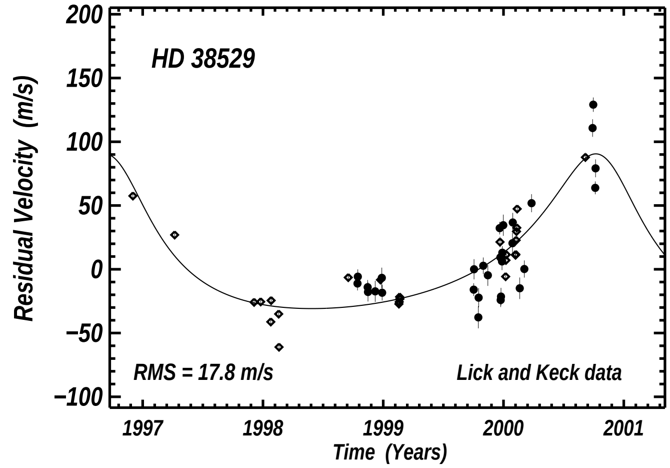

FIG. 8.—Residual radial velocities after subtracting the 14.3 day theoretical velocities for HD 38529. Interpreted as a dynamical effect, this curve suggests a minimum Keplerian solution for a second companion with $P > 1500$ days and a minimum $M \sin i$ of $\sim 4\, M_J$. Since the outer orbit has not yet closed, the period and mass of the second companion may be arbitrarily large.

declination of -4.17 ± 3.00 and 7.31 ± 2.09 mas yr^{-2}, respectively.

HD 38529 sits above the main sequence, so one concern is that this subgiant may have astrophysical sources for the velocity variations. A color-magnitude diagram of the Lick stars (Fig. 9) shows the position of HD 38529 relative to the rest of our sample. There are three other subgiants (HR 7602: $M = 1.27\, M_\odot$, $M_V = 3.03$ mag; HR 6869: $M = 1.41\, M_\odot$, $M_V = 1.84$ mag; and HR 8382: $M = 1.25\, M_\odot$, $M_V = 3.46$ mag) on the Lick target list. The relative radial velocities for these three subgiants are shown in Figure 10. The rms scatter in the velocities of HR 7602 (Fig. 10: *top panel*) is 10.3 m s^{-1} from 1987 to 2000. Velocities of HR 7602 after the Hamilton optics were upgraded have an rms scatter of 6.5 m s^{-1}. The rms scatter for HR 6869 (Fig. 10: *middle*

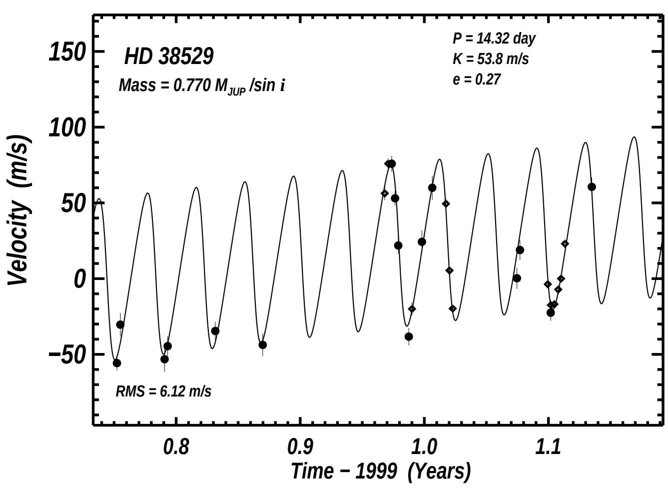

FIG. 7.—Combined Lick and Keck radial velocities HD 38529 during 6 months that reveal the 14.3 day periodicity. The velocities are modulated by a long-term trend. Lick observations are shown as circles, and the Keck data are plotted as diamonds. The solid line shows the Keplerian curve plus a linear trend for the best-fit orbital solution.

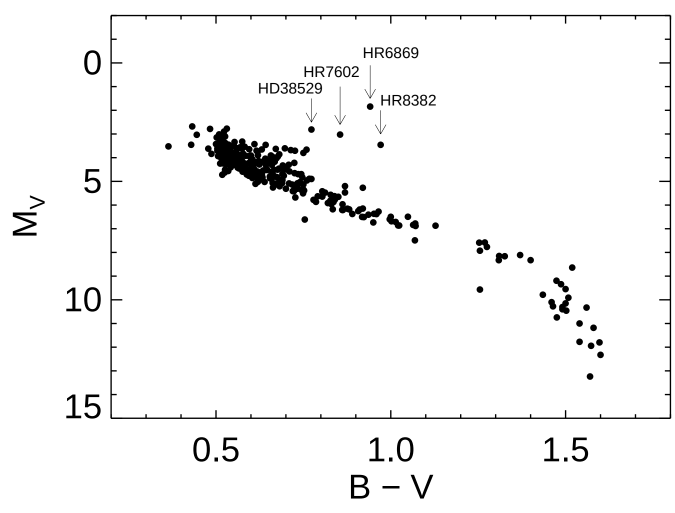

FIG. 9.—Color-magnitude diagram of target stars on the Lick planet search project. The position of HD 38529 is indicated, along with three other subgiants in our program: HR 7602, HR 6869, and HR 8382. These latter three subgiants yield rms velocities of ~ 5 m s^{-1} despite their slightly evolved status, suggesting that the excess velocity variations in HD 38529 are dynamical.

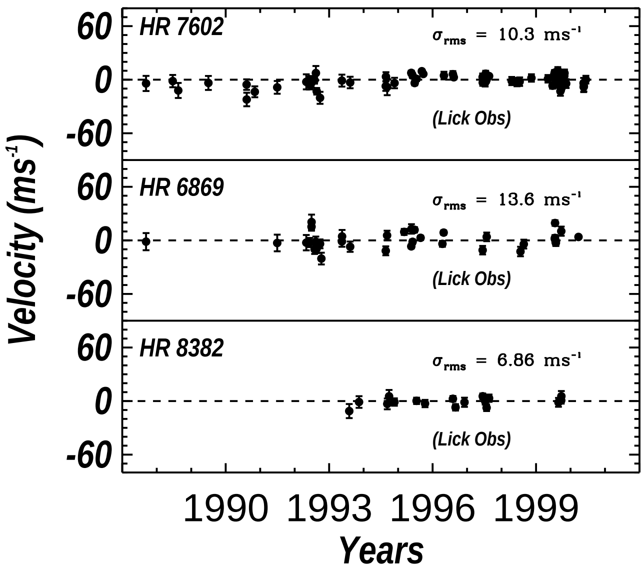

FIG. 10.—Montage of relative velocity plots for subgiants HR 7602, HR 6869, and HR8382. The single-measurement velocity precision for these stars is typically 4–5 m s^{-1}. The improvement in the velocity precision after the upgrade of the Hamilton optics at Lick in 1994 November is apparent.

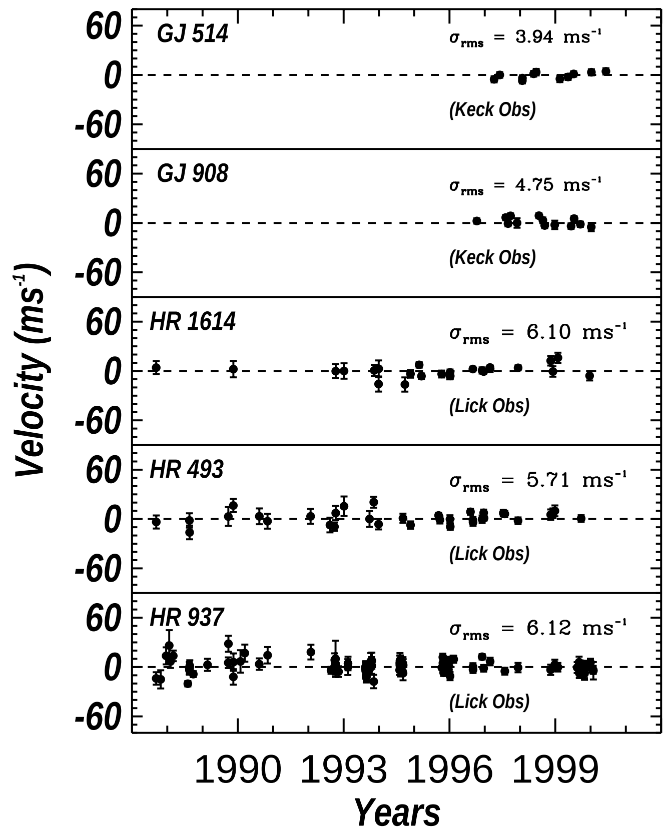

FIG. 11.—Relative velocities of five standard stars from Keck and Lick. The precision at Lick before 1994 is $\sim$10 m s^{-1} and afterward is $\sim$5 m s^{-1}.

panel) is 13.6 m s^{-1}, with a postupgrade rms scatter of 8 m s^{-1}. The data for HR 8382 extend from 1993 to 2000 (Fig. 10: *bottom panel*). The rms scatter is 6.86 m s^{-1}, and the postupgrade rms scatter is less than 4.5 m s^{-1}. None of these subgiants show periodicity in a periodogram analysis of their radial velocities, and the low rms scatter and low internal error bars suggest that astrophysical noise is typically less than 10 m s^{-1} for subgiants in this part of the color-magnitude diagram.

3. VARIATIONS IN KEPLERIAN RESIDUALS OF KNOWN EXTRASOLAR PLANETS

As part of our program, we obtain nightly observations of stars that we have classified as standard stars. These chromospherically inactive stars exhibit an internal velocity precision of 3–5 m s^{-1} and rms scatter less than 7 m s^{-1} during the 3–10 years that they have been observed. The standard stars provide a control group to judge the reality of variations in the velocity residuals of Keplerian fits.

Velocities for a few typical, standard stars are shown in Figure 11 (HR 7602 and HR 8382, shown in Fig. 10, are also considered standard stars in our Doppler program). The top two panels in Figure 11 show Keck standard stars (GJ 514 and GJ 908) with an rms scatter of about 4 m s^{-1} over the 3 yr time baseline of observations. The lower three panels in Figure 11 show Lick velocities for HR 1614, HR 493, and HR 937. These are typical standard stars with an rms scatter of about 6 m s^{-1} over the last decade. The improvement in the internal precision and lower rms velocity scatter in data obtained after revision of the Hamilton optics at Lick in 1994 are readily apparent to the eye.

For stars with known planets, we can check the orbital fit and identify additional velocity variations by subtracting the theoretical Keplerian velocities and examining the residual velocities. We consider here the sample of stars with (1) more than two years of data from Lick and (2) one announced planet. The 2 yr time baseline is arbitrary; however, for stars with one close companion, we expect that this longer time baseline is needed to assess the presence of a residual trend. There are 12 stars that meet these criteria. The characteristics of these stars, along with characteristics of the new planet-bearing stars HD 12661 and HD 92788, are noted in Table 5.

Six of the 12 stars with known planets have essentially constant residual velocities. Figure 12 shows the residual velocities (i.e., observed velocities with theoretical orbital velocities subtracted) for the stars 51 Peg (Mayor & Queloz 1995; Marcy et al. 1997), HD 195019 (Fischer et al. 1999), ρ CrB (Noyes et al. 1997), 70 Vir (Marcy & Butler 1996), 16 Cyg B (Cochran et al. 1997), and 47 UMa (Butler & Marcy 1996). The residual velocities for these six stars with known planets look very much like the Doppler velocities for our standard stars, with long-term rms scatter that is typically 7 m s^{-1} or less. In the case of HD 195019, only the higher-precision Keck velocities are shown. There is a low-amplitude systematic trend in the residual velocities for 47 UMa that we will continue to monitor with high-precision observations. However, if there are any additional planets orbiting these six stars, they may fall below our current detection threshold.

Five stars show coherent variations in their residual velocities, consistent with the interpretation of another companion in the system. These variations can be fitted with a long-period Keplerian, but the orbit has not yet closed (except for the case of Upsilon Andromedae), so we can only estimate minimum values for the orbital period and companion mass. The stars Upsilon Andromedae

TABLE 5

STELLAR CHARACTERISTICS

Star	M_* ($M_\odot$)	P (days)	M sin i (M_J)	e	[Fe/H]	log R'_{HK}	Residual Trend?
Tau Bootis	1.3	3.3126	4.14	0.02	0.32	−4.75	Yes
51 Pegasi	1.06	4.231	0.46	0.01	0.21	−5.03	No
Ups Andromedae b	1.3	4.617	0.68	0.02	0.12	−4.84	Yes
HD 217107	0.98	7.128	1.29	0.14	0.30	−5.09	Yes
55 Cancri	1.03	14.656	0.93	0.03	0.45	−4.91	Yes
HD 38529	1.4	14.31	0.76	0.27	0.29	−4.89	Yes
HD 195019	1.02	18.21	3.55	0.01	0.00	−4.90	No
Rho Coronae Borealis	0.95	39.81	0.99	0.07	−0.29	−5.02	No
GJ 876	0.32	60.0	2.18	0.25	...	...	Maybe
70 Virginis	1.10	116.7	7.42	0.402	−0.03	−5.06	No
HD 12661[a]	1.07	250.2	2.83	0.20	0.29	−5.12	Maybe
HD 92788[a]	1.06	337.7	3.86	0.28	0.22	−5.04	No
16 Cygni B	1.02	796.7	1.68	0.68	0.09	−4.98	No
47 Ursae Majoris	1.03	1097.0	2.63	0.115	−0.08	−4.99	Maybe

[a] Insufficient data to assess presence of a residual velocity trend.

(Butler et al. 1997, 1999), Tau Boo (Butler et al. 1997), 55 Cnc (Butler et al. 1997), and HD 217107 (Fischer et al. 1999) show velocity variations that are discussed individually below. Because the variations imply the existence of long periods, they are interesting targets for follow-up observations with adaptive optics and the *Hubble Space Telescope* (*HST*). One star, GJ 876 (Marcy et al. 1998), shows velocity variations for which we cannot identify a coherent periodicity.

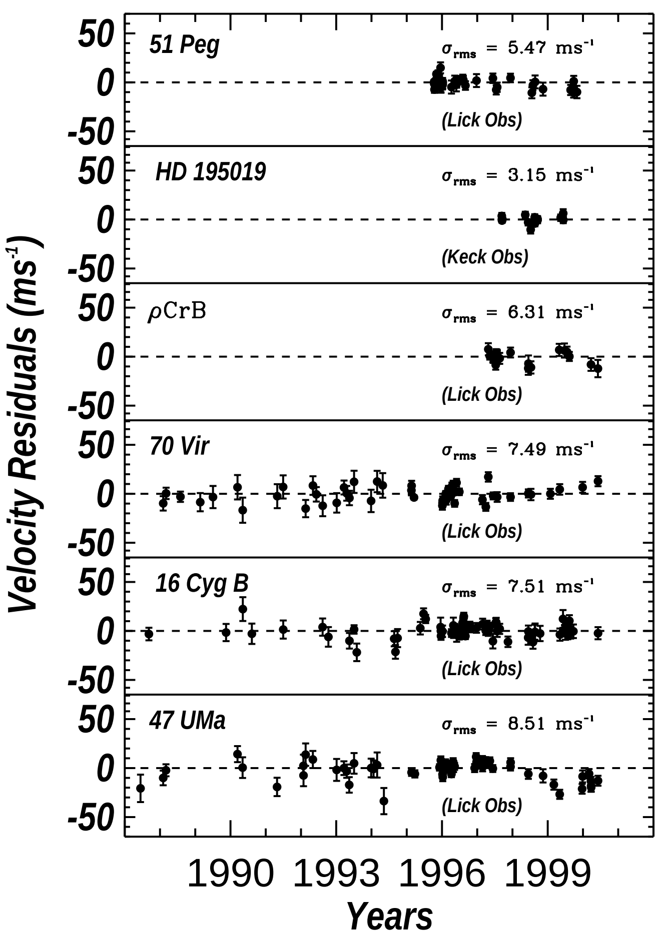

FIG. 12.—Flat residual velocities of six stars with detected planets. The rms is typically 7 m s^{-1}, and no trends are observed.

3.1. *Upsilon Andromedae*

Three companions to the F8V star Upsilon Andromedae were identified by Butler et al. (1999). In Figure 13, we update the residual velocities (after subtraction of the inner planet) with an additional year of intensely sampled velocities from Lick. The three-planet solution continues to fit the data well, with residuals that exhibit an rms of 10.7 m s^{-1}, consistent with velocity errors (9 m s^{-1}) and expected intrinsic photospheric noise for this rapidly rotating star ($v \sin i \sim 9$ km s^{-1}). This rms has improved from 15 m s^{-1} in the published fit because of dense sampling and the resulting improved Keplerian model.

We do not see indications of any additional velocity variations beyond those caused by the previously announced three planets. The closest planet in this system

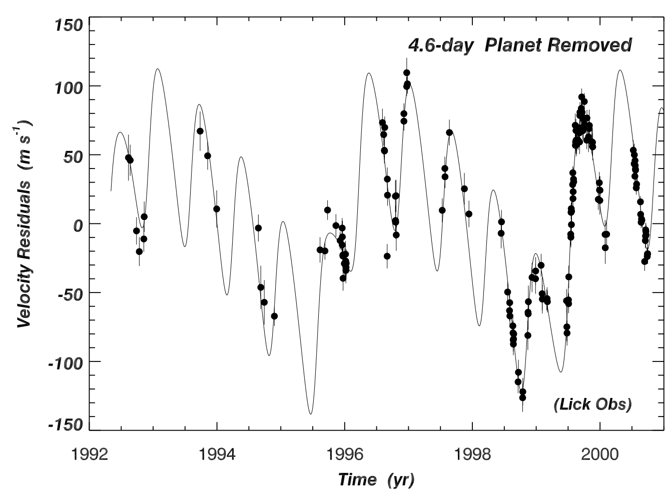

FIG. 13.—Residual velocities to Upsilon Andromedae after subtracting the velocities caused by the 4.167 day planet. Velocity modulation by two dynamical companions can be seen in the data. The solid line represents the theoretical velocity variations due to the outer two planets, obtained by a self-consistent fit to all three companions followed by subtraction of effects of the 4.167 day planet.

resides in an orbit with $P_b = 4.617 \pm 0.001$ days, $e_b = 0.01 \pm 0.01$, and $K_b = 71.0 \pm 1.6$ m s^{-1}. The revised orbital elements for the middle companion are $P_c = 240.6 \pm 1.0$ days, $e_c = 0.23 \pm 0.015$, $K_c = 57.4 \pm 1.6$ m s^{-1}, and $\omega_c = 240\overset{\circ}{.}6 \pm 3°$. The revised orbital solution for the outer planet is $P_d = 1314.5 \pm 5$ days, $e_d = 0.35 \pm 0.02$, $K_d = 68.6 \pm 1.8$ m s^{-1}, and $\omega_d = 234\overset{\circ}{.}5 \pm 3°$. The major axes of the outer two planets are nearly aligned, perhaps related to a secular resonance between them, which may bear on the formation and dynamical stability of the system (Laughlin & Adams 1999; Mardling & Lin 2000; Rivera & Lissauer 2000).

The discovery process of the long-period planets around Upsilon Andromedae provides insight into the interpretation of residuals of other stars. In the case of Upsilon Andromedae, a long-period trend was noted a year after the closest planet was discovered. The velocity variation was coherent, but with additional scatter (later understood as velocity variations from the unanticipated middle planet), and it was significant at the several σ level. The rms scatter in the orbital fit was initially high until additional data allowed us to extract a better Keplerian fit. Quantitatively and qualitatively, the residual trends that we see in HD 38529, τ Boo, 55 Cnc, and HD 217107 bear a resemblance to the residual velocity variations that emerged in Upsilon Andromedae. All exhibit coherent, several σ variations, but not closure of a Keplerian orbit.

3.2. *Tau Boo*

Tau Boo has a known planetary companion with an orbital period of 3.313 days. Observations of this star extend back to 1987, and a shallow trend in the residual velocities (Fig. 14) is apparent. The internal errors for velocities obtained between 1990 and 1994 (before the upgrade to the Hamilton optics) are particularly large for unknown reasons. This F7 V star has a $v \sin i$ of 15 km s^{-1} (Baliunas et al. 1997), which contributes to the typical errors of 20 m s^{-1} in the post-fix velocities.

Fitting a Keplerian to the data suggests a possible second companion with an orbital period longer than 20 yr and an $M \sin i$ greater than ~ 15 M_J. This fit gives an rms that is 10 m s^{-1} lower than that of a linear fit, largely because the velocities from 1987 to 1990 have a slightly positive slope. The postupgrade velocities from 1995 to 2000 have a linear slope of -15 m s^{-1} yr^{-1} with rms scatter to the linear fit of 16.5 m s^{-1}, consistent with our single measurement errors.

Tau Boo is a visual binary with an M2V companion. The projected separation (Gliese & Jahreiss 1979) has decreased from 10''.3 in 1849 to 5''.4 in 1958. Adaptive optics at the Lick Observatory in 1999 July (Lloyd et al. 2001) reveal an angular separation of 2''.85, and 10 μm observations from 1998 January show a 3''.04 separation (P. Kalas 2000, private communication). At a distance of 15.6 pc, this implies a projected linear separation of 44 AU between τ Boo and the M dwarf companion. If the 1988–1990 velocity measurements of τ Boo are systematically low, the residual velocities could be interpreted as a linear trend originating from the M dwarf companion.

3.3. *55 Cnc*

The G8V star 55 Cnc has a known planetary companion with an orbital period of 14.67 days (Butler et al. 1996). Marcy & Butler (1998) noted a trend in the residual velocities consistent with a second companion. The residual velocities, updated in Figure 15 with two more years of data, remain consistent with a dynamical interpretation. Fitting the residuals with a Keplerian suggests that this companion has an orbital period greater than 12 yr and a mass of at least 3.2 M_J. As with τ Boo, the estimate for $M \sin i$ is a minimum because the Keplerian curve has not yet closed. Since $M \sin i$ could be significantly higher than a few M_J, and the implied separation is 5.5 AU, or 0''.44, this would also be an interesting target for adaptive optics or the *HST*.

The rms scatter in the residual velocities about the residual trend is 12.1 m s^{-1}, or 3 times the average internal error bars of our observations, similar to the large rms scatter in HD 38529. The rotation period of this late-type G dwarf, suggested from Ca II H and K emission, is about 42 days. Baliunas et al. (1997) observe modulation of the Ca II H and K lines over three seasons having a mean period of 41.7 days and varying amplitude, which they interpret as rotational modulation. A periodogram analysis of our twice-detrended velocities (Fig. 16) shows a moderately

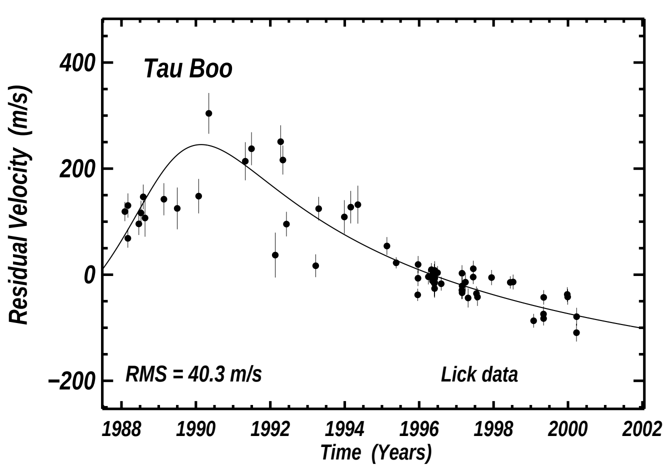

FIG. 14.—Residual velocities for Tau Boo. The apparent variation is consistent with a companion in an orbital period longer than ~ 20 yr and mass greater than ~ 15 M_J. It is possible that the nearly linear residual velocity trend stems from a nearby M dwarf companion.

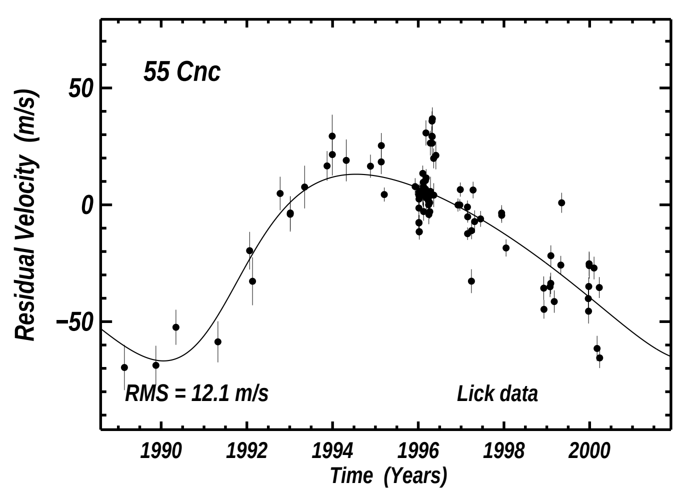

FIG. 15.—Residual velocities for 55 Cnc. The minimum Keplerian solution to the residual velocity variations suggest the presence of a companion having orbital period greater than 10 yr and mass greater than $M \sin i = 3.4$ M_J. The reality of this interpretation awaits phase closure.

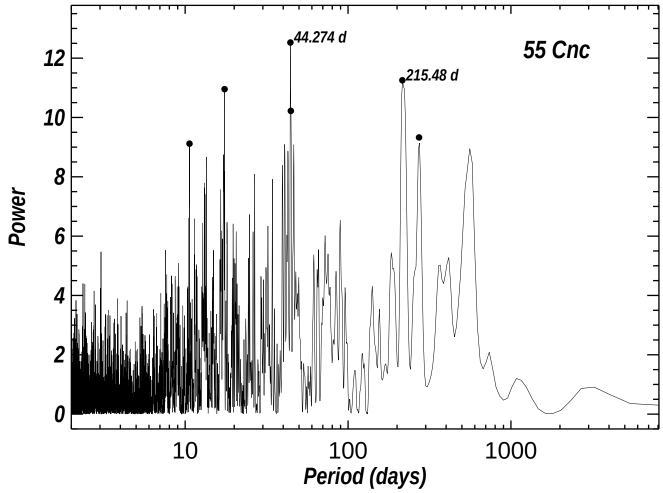

FIG. 16.—Periodogram of doubly detrended velocities for 55 Cnc. No clear additional period appears. The peak at $P = 44$ days may correspond to rotation of surface features.

strong peak at 44 days, which may be due to rotation of active regions on the surface of the star, although the amplitude of this periodicity is too low to model with our current data set. Again, any errors in the orbital model for this

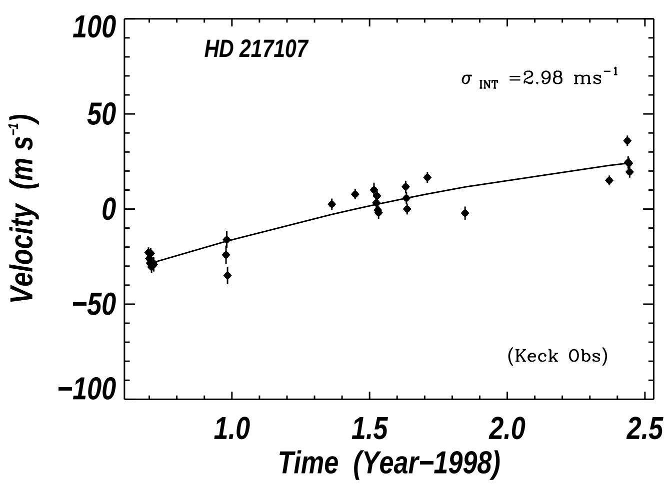

FIG. 17.—Residual velocities for HD 217107, showing a trend

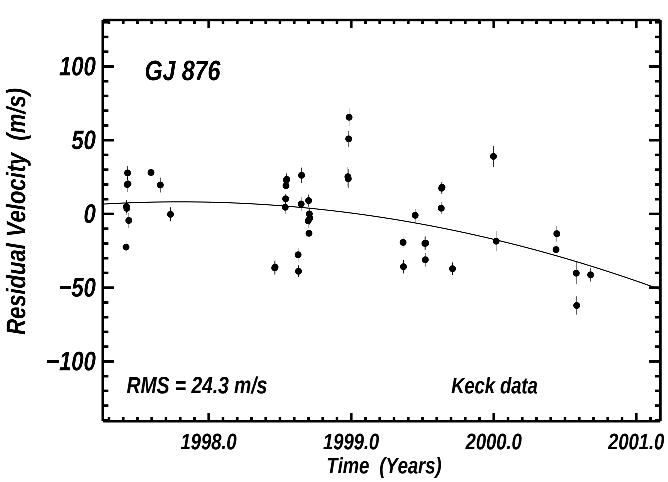

FIG. 18.—Residual velocities for GJ 876, which exhibit unusually large scatter at the 24 m s^{-1} level.

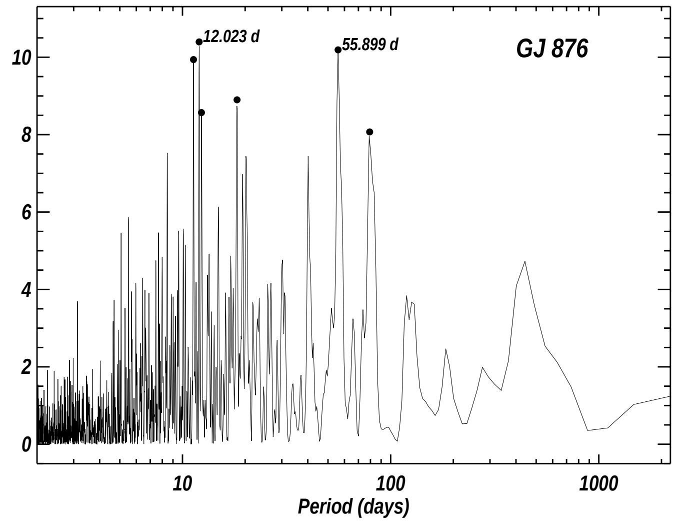

FIG. 19.—Periodogram of the residual velocities for GJ 876. No clear additional period appears.

two-planet fit would translate into increased rms scatter of the magnitude that we observe here.

3.4. *HD 217107*

HD 217107 (G8V) harbors a planet with $M \sin i = 1.3$ M_J and an orbital period of 7.13 days (Fischer et al. 1999). Extrasolar planets with orbital periods closer than 10 days tend to reside in circular orbits, with two exceptions: HD 217107 and HD 108147. The orbital solution for HD 217107 yields an eccentricity $e = 0.14 \pm 0.02$ and interestingly shows a strong linear trend of 38.2 m s^{-1} yr^{-1} in the residuals of the combined Lick and Keck data (and in each of the data sets individually). The unusual eccentricity of the inner planet may be physically induced by an additional perturbing companion in the system.

Figure 17 shows that there is only a hint of curvature in the velocities for this star. Under the roughest estimate that the orbital period will be at least 3 times the length of the observed velocities, the implied semimajor axis for the suspected second companion would be greater than a few AU ($>0''.17$), and $M \sin i$ would be greater than 3 M_J. Adaptive optics and *HST* observations for this star are warranted.

3.5. *GJ 876*

The M4V star, GJ 876, has a known planet with $M \sin i = 4.6$ M_J in a 60 day orbit (Delfosse et al. 1998; Marcy et al. 1998). The typical velocity precision for GJ 876 is 4.6 m s^{-1} at Keck. However, after removing the theoretical velocity curve for the known planet, the residual velocity variations have an rms = 24 m s^{-1} (Fig. 18). There is no long-term curvature apparent to the eye in the three years of residual Keck velocities or in the seven years of lower precision Lick velocities. A periodogram analysis of the Keck residual velocities (Fig. 19) does not show a dominant peak. We do not see similar velocity scatter among the many other M dwarfs on the Keck project (Fig. 11). (See the note added in proof at the end of this paper.)

4. DISCUSSION

Precision Doppler observations at Lick and Keck have revealed planetary companions to the stars HD 12661, HD

92788, and HD 38529. Similar to other Doppler-detected planets that orbit beyond 0.2 AU, all of these extrasolar planets reside in eccentric orbits. All three stars appear to be metal-rich relative to field stars, further strengthening the correlation between the presence of gas giant planets and high metallicity in host stars.

HD 12661 is typical of extrasolar planets discovered to date, with $M \sin i = 2.83\ M_J$, an orbital period of 250.2 days, and an eccentricity of 0.20. HD 92788 is similarly typical, with an orbital period of 337.7 days, an eccentricity $e = 0.28$, and a companion mass $M \sin i = 3.86\ M_J$. Our best Keplerian solution suggests that there is a residual velocity trend for this star.

HD 38529 has a more complicated velocity pattern that suggests the presence of more than one companion. There is a short-period Keplerian velocity variation of 14.3 days, which we attribute to a companion with $M \sin i = 0.77\ M_J$. However, during the 3 yr timespan of data, the velocities for HD 38529 show additional variation with significant curvature. These residual variations for HD 38529 are similar to those observed for 55 Cnc and Upsilon Andromedae (prior to the discovery of its two additional planets). We must wait for closure of the long-period trend to assess the Keplerian nature of the velocities and to derive orbital parameters.

The observations of the residual variations for HD 38529 motivated us to assess how often such large residual variations occur. We examined the residual velocities for a sample of stars that had at least two years of Lick observations and one known planet. Twelve stars met these selection criteria, including the star HD 38529. For each of these 12 stars, we subtracted the velocities that could be attributed to the known planet and then examined the residual velocities for additional trends.

Six of the 12 stars (51 Peg, HD 195019, ρCrB, 70 Vir, 16 CygB, and 47 UMa) showed residual velocities with an rms scatter of about 7 m s^{-1}, consistent with a mixture of measurement errors and stellar noise. The remaining six of our 12 stars exhibit variations in the residuals that are greater than expected from errors or intrinsic stellar noise. Five of the 12 stars (τ Boo, Ups Andromedae, HD 217107, 55 Cnc, and HD 38529) exhibit coherent, long-period variations that are consistent with the presence of an additional companion in the system. In the case of τ Boo, the residual velocity trend may be attributable to the presence of a known M dwarf companion. The M4V star, GJ 876, is perhaps the most puzzling of the 12 stars. This star shows residual velocities of 24 m s^{-1} (a 6 σ result) in 49 Keck observations spanning three years. However, we do not see a second dominant periodicity in the Keck or Lick data at this time.

Thus, in our small sample of 12 systems, we find that 50% of the stars with one known planet show no evidence of a detectable additional companion, planetary or otherwise. However, five stars exhibit variations for which a plausible explanation remains an additional companion. This 42% rate of occurrence of velocity variations far exceeds that found in our single stars, since less than 10% of stars without detected planets show such variations in our sample. These occurrence rates suggest that the known planet-bearing stars harbor a distant ($a > 3$ AU) companion more often than the remaining target stars.

We note that the distant companions occur predominantly around stars with a short-period planet ($P < 15$ days) rather than a long-period planet. One wonders if this is a selection effect. Would the residual velocities that we observe for short-period planets around τ Boo, 55 Cnc, Ups Andromedae (d), and HD 217107 have been detected in the stars with longer-period planets? To investigate this, we added theoretical residual velocities to the stars with a known planet in an orbit longer than 15 days. The residual velocities we added were based on Keplerian fits to the residual velocities in τ Boo, 55 Cnc, Ups Andromedae (d), and HD 217107. Since some orbital phases are more detectable than others, we stepped through the theoretical second orbits by $\pi/4$ and tested detectability at each phase. Our first test was for the short-period system, 51 Peg, which shows constant residual velocities. We ran three trials, introducing the residual velocities seen in 55 Cnc at three different phase shifts of the suspected 12.3 yr second period. We then ran our Keplerian fitting routine to determine if we would recover both the known 4.23 day companion to 51 Peg and the injected companion. We repeated this experiment with the ensemble of residual variations observed for τ Boo, Ups Andromedae (d) and HD 217107.

In all trials, we were able to recover the known companion with an orbital period that was very close to the orbital period detected without an artificial trend added. However, the other orbital elements (notably, eccentricity) often changed since the least-squares minimization algorithm absorbed varying amounts of the simulated residual variation. We were able to detect the injected residual velocity variations in all cases for 70 Vir and for 51 Peg, which have been observed with high cadence for several years. However, the additional variations were not detected, after solving for the known companions, for HD 195019 and ρ CrB (which have shorter baselines of observations) in most trials. The Keplerian solution for the detected, inner planet tends to absorb the effects of the hypothetical, outer companion, diminishing the detectability of additional distant planets.

To date, all of the extrasolar planets detected in orbits with semimajor axes greater than 0.2 AU appear to have orbital eccentricities greater than those of the giant planets in our own solar system. In simulations where a second artificial companion was added to the velocities, the best-fit orbital eccentricity of the known companion was (spuriously) increased by amounts ranging from 0.02 to 0.25. The increase in absorbed eccentricity was smallest for those data sets with good sampling (several observations per year and a time baseline of more than 4 yr). The increase in orbital eccentricity was also small for cases where a linear trend was allowed in the Keplerian fit. Velocity errors, poor phase coverage, and unresolved trends all serve to increase the derived eccentricity. It is rare for these effects to conspire in such a way to decrease eccentricity. The key to determining accurate eccentricity is dense phase coverage and high-velocity precision. These conditions are most likely to be met for the stars with the shortest period planets (3–15 days), and indeed, these are the systems in which we have detected residual velocity variations. If additional long-period planets exist, there is a detectability challenge that may bias us against discovering these companions. This bias is compounded by the additional challenge of detecting the intrinsically small-velocity amplitude induced by a more distant planet.

We dedicate this work to the memory of our friend and coworker, Jim Burrous. We gratefully acknowledge the efficiency and dedication of the Lick Observatory staff, including Tony Misch, Keith Baker, Kostas Chloros, Wayne Earthman, John Morey, and Andy Tullis. We thank Doug Lin, Greg Laughlin, Mike Liu, James Lloyd, and Paul Kalas for useful conversations and insights. We acknowledge support from NASA grant NAG 5-75005 (to G. W. M.), NSF grant AST 96-19418 and NASA grant NAG 5-4445 (to S. S. V.), and Sun Microsystems. We thank the NASA and University of California Telescope assignment committees for allocations of telescope time. This research has made use of the Simbad database, operated at the Centre de Données astronomiques de Strasbourg, France.

REFERENCES

Baliunas, S. L., Donahue, R. A., Soon, W., & Henry, G. W. 1998, in ASP Conf. Proc. 154, Cool Stars, Stellar Systems and the Sun, ed. R. A. Donahue & J. A. Bookbinder (San Francisco: ASP), 153
Baliunas, S. L., et. al. 1995, ApJ, 438, 269
Baliunas, S. L., Henry, G. W., Donahue, R. A., Fekel, F. C., & Soon, W. H. 1997, ApJ, 474, L119
Butler R. P., & Marcy, G. W. 1996, ApJ, 464, L153
Butler, R. P., Marcy, G. W., Fischer, D. A., Brown, T. M., Contos, A. R., Korzennik, S. G., Nisenson, P., & Noyes, R. W. 1999, ApJ, 526, 916
Butler, R. P., Marcy, G. W., Vogt, S. S., & Apps, K. A. 1998, PASP, 110, 1389
Butler, R. P., Marcy, G. W., Williams, E., Hauser, H., & Shirts, P. 1997, ApJ, 474, 115L
Butler, R. P., Marcy, G. W., Williams, E., McCarthy, C., Dosanjh, P., & Vogt, S. S. 1996, PASP, 108, 500
Charbonneau, D., Brown, T. M., Latham, D. W., & Mayor, M. 2000, ApJ, 529, 45L
Cochran, W. D., Hatzes, A. P., Butler, R. P., & Marcy, G. W. 1997, ApJ, 483, 457
Delfosse, X., Forveille, T., Mayor, M., Perrier, C., Naef, D., & Queloz, D. 1998, A&A, 338, L67
Fischer, D. A., Marcy, G. W., Butler, R. P., Vogt, S. S., & Apps, K. 1999, PASP, 111, 50
Gliese, W., & Jahreiss, H. 1979, A&AS, 38, 423
Henry, G. W., Marcy, G. W., Butler, R. P., & Vogt, S. S. 2000, ApJ, 529, 41L
Laughlin, G., & Adams, F. C. 1999, ApJ, 526, 881
Lloyd, J. P., et al. 2001, in IAU Symp. 202, Planetary Systems in the Universe, ed. A. J. Penny, P. Artmymowicz, A. M. Lagrange, & S. S. Russell (San Francisco: ASP), in press
Marcy, G. W., & Butler R. P. 1996, ApJ, 464, L147
———. 1998, ARA&A, 36, 57
Marcy, G. W., Butler, R. P., Vogt, S. S., Fischer, D. A., & Lissauer, J. 1998, ApJ, 505, L147
Marcy, G. W., Butler, R. P., Vogt, S. S., Fischer, D. A., & Liu, M. 1999, ApJ, 520, 239
Marcy, G. W., Butler, R. P., Williams, E., Bildsten, L., Graham, J. R., Ghez, A., & Jernigan, G. 1997, ApJ, 481, 926
Marcy, G. W., Cochran, W. D., & Mayor, M. 2000, in Protostars and Planets IV, ed. V. Mannings, A. P. Boss, & S. S. Russell (Tucson: Univ. Arizona Press), 1285
Mardling, R. A., & Lin, D. N. C. 2000, ApJ, submitted
Mayor, M., & Queloz, D. 1995, Nature, 378, 355
Noyes, R. W., Hartmann, L., Baliunas, S. L., Duncan, D. K., & Vaughan, A. H. 1984, ApJ, 279, 763
Noyes, R. W., Jha, S., Korzennik, S. G., Krockenberger, M., Nisenson, P., Brown, T. M., Kennelly, E. J., & Horner, S. D. 1997, ApJ, 483, L111
Perryman, M. A. C. 1997, The Hipparcos and Tycho Catalogs (ESA-SP 1200; Noordwijk, Netherlands)
Prieto, A., & Lambert, D. L. 1999, A&A, 352, 555
Queloz, D., Mayor, M., Naef, D., Pepe, F., Santos, N. C., Udry, S., & Burnet, M. 2001, in IAU Symp. 202, Planetary Systems in the Universe: Observation, Formation and Evolution, ed. A. J. Penny, P. Artymowicz, A. M. Lagrange, & S. S. Russell (San Francisco: ASP), in press
Radick, R. R., Lockwood, G. W., Skiff, B. A., & Baliunas, S. L. 1998, ApJS, 118, 239
Rivera, E. J., & Lissauer, J. J. 2000, ApJ, 530, 454
Saar, S. H., Butler, R. P., & Marcy, G. W. 1998, ApJ, 498, L153
Udry, S., Mayor, M., Queloz, D. 2001, in IAU Symp. 202, Planetary Systems in the Universe: Observation, Formation and Evolution, ed. A. J. Penny, P. Artymowicz, A. M. Lagrange, & S. S. Russell (San Francisco: ASP), in press
Vogt, S. S. 1987, PASP, 99, 1214
Vogt, S. S., Marcy, G. W., & Butler, R. P., & Apps, K. 2000, ApJ, 536, 902

Note added in proof.—An additional planetary companion to GJ 876 (Marcy et al., ApJ, in press [2001]) in a 2:1 resonance orbit has been identified, which accounts for the scatter in residual velocities noted in this paper. In addition, the velocity phased closed for the outer companion to HD 168443 (Marcy et al., ApJ, in press [2001]).